

## Effects of Pauli's Principle in the $\alpha$ - $^{16}\text{O}$ Elastic Scattering

H. SCHECHTER, L.F. CANTO and A.M. BREITSCHAFT

*Instituto de Física, Universidade Federal do Rio de Janeiro, Caixa Postal 68528, Rio de Janeiro, 21944, RJ, Brasil*

Recebido em 11 de outubro de 1985

**Abstract** "Exact" microscopic methods like the RGM (Resonating Group Method) and the GCM (Generator Coordinate Method) and approximate methods like the OCM (Orthogonality Condition Model) are used to study the effects of Pauli's Principle in the  $\alpha$ - $^{16}\text{O}$  elastic scattering. A method to derive "exact" effective potentials for the OCM is introduced. These potentials, derived from RGM wave functions, make the OCM identical to the RGM and they have the advantage of being free from poles associated to the forbidden states. Numerical calculations are made with V2 and B1 nucleon-nucleon forces at energies in the range 0-30 MeV. The potentials and the resulting phase-shifts are compared to those obtained from the approximate method suggested by Friedrich and Canto. The problem of searching for local, state independent, potentials for the OCM is discussed.

### 1. INTRODUCTION

In recent times, the microscopic treatment of elastic scattering between light nuclei has gone through considerable progress in two ways mainly: first, exact microscopic theories like the RGM<sup>1</sup> and the GCM<sup>2</sup> became more treatable by the development of new methods<sup>3,4</sup> of attacking the crucial problem of these theories, vis, the calculation of their kernels; second, approximate methods which avoid kernel calculation, like the OCM<sup>5</sup>, became more sophisticated and are being applied<sup>6-8</sup> to a great number of systems.

The present work studies some aspects of the OCM in connection with the  $\alpha$ - $^{16}\text{O}$  system. In an earlier work<sup>9</sup> we applied the microscopic method of ref. 7 to  $\alpha$ - $^{16}\text{O}$  scattering, using a Volkov<sup>12</sup> V2 nucleon-nucleon interaction. Here, we develop a method to derive local effective potentials directly from RGM wave functions, and apply it to the  $\alpha$ - $^{16}\text{O}$  system, comparing the results to those of ref. 9. This method has the advantage of allowing the elimination of poles in the potential arising from the orthogonality of the RGM wave function to the redundant states. Such comparison may guide the effort to find a simple potential that,

being local, represent the interaction between nuclei in the best possible way.

In section 2 we show how to derive our "exact" effective potentials, and discuss the problems related to them. In section 3 we use the method of section 2 to calculate effective potentials for the  $\alpha$ - $^{16}\text{O}$  system. In section 4 we compare phase-shifts obtained with "exact" and approximate effective potentials in Saito's OCM equation and discuss possible ways to improve the approximate method. Finally, the conclusions of the present work are presented in section 5.

## 2. DERIVATION OF EFFECTIVE POTENTIALS FOR SAITO'S EQUATION

Saito's OCM equation,

$$\Lambda_\ell (T_\ell + V_D) \chi_\ell(x) = \epsilon \chi_\ell(x) \quad (1)$$

furnishes a wave function  $\chi_\ell(x)$  which gives an approximate description of the relative motion of the nuclear fragments.  $\epsilon$  is the energy of the relative motion of the fragments and  $T_\ell$  is the kinetic energy operator

$$T_\ell = - \left( \frac{\hbar^2}{2\mu} \right) \left[ \frac{d^2}{dx^2} - \frac{\ell(\ell+1)}{x^2} \right] ; \quad (2)$$

$\Lambda_\ell$  is the operator

$$\Lambda_\ell = 1 - \sum_n |\phi_{n,\ell}^0\rangle \langle \phi_{n,\ell}^0| , \quad (3)$$

which eliminates from the wave functions any components in the subspace spanned by the forbidden states  $|\phi_{n,\ell}^0\rangle$ , eigenstates of  $\Lambda_\ell$  with null eigenvalues.

As it was discussed in refs. 6,9, Saito's equation becomes equivalent to the RGM when one replaces the direct RGM potential  $V_D$  by a properly chosen effective potential  $V_{\text{ef}}$ . Along these lines Friedrich and Canto<sup>7</sup> proposed a simple method to derive a local, state independent, approximation for  $V_{\text{ef}}$ . In their method the effective potential is parametrized in a simple form and the parameters are determined by fitting a fundamental relation involving  $V_{\text{ef}}$  and CGM Kernels. Their method was applied<sup>7-10</sup> to the scattering of light nuclei up to  $^{48}\text{Ca}$  with variable

degrees of success. In some of these cases angular momentum<sup>8</sup> or parity<sup>9,10</sup> dependence was introduced in  $V_{ef}$  for the sake of obtaining more realistic results.

The starting point of our method to derive an "exact" effective potential is the basic relation<sup>6,9</sup>

$$H = A^{1/2} (T + V_{ef}) A^{1/2}, \quad (4)$$

where  $H$  is the RGM Hamiltonian Kernel for the relative motion of the fragments and  $A^{1/2}$  is the Hermitian "square root" of the RGM overlap Kernel, determined by the operators equation

$$A^{1/2} A^{1/2} = A \quad (5)$$

Equation (4) determines a family of potentials which makes the OCM exactly equivalent to the RGM. The potentials have, in principle, complicated non-local forms. If we wish to keep, however, the spirit of the OCM, we must look for the best local approximation for  $V_{ef}$ .

Within this perspective we use RGM wave functions in the "inverse direction", that is, we calculate effective potentials from RGM "exact" wave functions  $g_{\ell,\epsilon}$  obtained from an RGM/GCM code<sup>11</sup>. We build the renormalized RGM wave function

$$\chi_{\ell,\epsilon} = A_{\ell}^{1/2} g_{\ell,\epsilon} \quad (6)$$

and assume that it is an exact solution of Saito's equation. Using (6) and the explicit form of the projector  $\Lambda_{\ell}$  in Saito's equation we get

$$V_{ef} = V_{\ell,\epsilon}(x) = \left[ (\epsilon - T_{\ell}) \chi_{\ell,\epsilon}(x) + \sum_{n=0}^{n_0-1} \phi_{n,\ell}^0(x) \cdot d_{n,\ell} \right] / \chi_{\ell,\epsilon}(x), \quad (7)$$

where  $\phi_{n,\ell}^0(x)$  are the forbidden states wave functions. The coefficients  $d_{n,\ell}$  are formally given by

$$d_{n,\ell} = \langle \phi_{n,\ell}^0 | T_{\ell} + V_{\ell,\epsilon} | \chi_{\ell,\epsilon} \rangle, \quad (8)$$

but they are in fact arbitrary since the projector  $\Lambda_{\ell}$  in equation (1) annihilates the corresponding term in the product  $V_{\ell,\epsilon}(x) \cdot \chi_{\ell,\epsilon}(x)$ . As the number of nodes arising from the orthogonality of  $\chi_{\ell,\epsilon}$  to the for-

bidden states is equal to the number of coefficients  $d_{n,\ell}$ , these coefficients can be chosen so that the numerator in the right hand side of (7) vanishes at these nodes.

With this procedure all poles of  $V_{ef}$  resulting from the orthogonality of  $\chi$  to the forbidden states can be eliminated. On the other hand, other poles associated to oscillations of the asymptotic wave function will remain.

We should have in mind that the local form of  $V_{ef}$  may be rather artificial, since it was imposed "a priori". If that is the case, the non-local nature of the potential emerges as a strong dependence on the RGM wave function used in its determination. Thus, we can learn about residual effects of the antisymmetrization by investigating the state dependence of  $V_{ef}$ .

### 3. CALCULATION OF EFFECTIVE POTENTIALS. APPLICATION TO $\alpha$ - $^{16}\text{O}$ SCATTERING

We have calculated the effective potentials established in section 2 for  $\alpha$ - $^{16}\text{O}$  scattering, using two nucleon-nucleon interactions: the Volkov force  $V2$ <sup>12</sup> and the Brink-Boeker force  $B1$ <sup>13</sup>. Single particle orbitals were described by harmonic oscillator wave functions with oscillator lengths  $b = 1.62$  fm and  $b = 1.77$  fm, in the  $V2$  and  $B1$  cases, respectively. In what follows we will give only the nuclear part of the effective potentials. This is done approximately<sup>9</sup> by subtracting the direct RGM Coulomb Kernel from the total effective potential.

Effective potentials were calculated using eq. 7 at the energies  $E = 3$  MeV, 9 MeV, 15 MeV, 21 MeV for values of angular momentum  $\ell = 0, 1, \dots, 9$ . Table 1 illustrates the behaviour of the potentials for some partial waves. For both interactions one notices a pronounced dependence on parity and a weaker dependence on energy and angular momentum among states of the same parity. These facts suggest the setting up of potentials  $\bar{v}^{(\pm)}(r)$  representing, on the average, the potentials of table 1 for the parities (+) and (-). These potentials are represented in fig. 1 by dashed lines.

A special situation occurs at resonance energies or bound states of the system. In such cases, the wave function has a very large amplitude in the inner region, and the matching to its appropriate

Table Ia - Nuclear part of the effective potentials (in MeV) for the  $\alpha$ - $^{16}\text{O}$  system with a V2 interaction at center-of-mass energies: a) 9 MeV, b) 15 MeV and c) 21 MeV. Inaccurate values of the potential near poles are replaced by an asterisk.

(a)

$x/b$	$\ell = 0$	1	2	3	4	5
0.5	-137.6	-130.0	-137.3	-128.4	-136.4	-126.0
1.5	-89.8	-87.3	-89.5	-86.2	-88.8	-84.2
2.5	*	-26.1	*	-25.7	*	-25.0
3.5	-4.0	-4.7	-4.2	-4.8	-4.4	-5.3

(b)

$x/b$	$\ell = 0$	1	2	3	4	5
0.5	-136.2	-132.5	-137.8	-131.1	-137.0	-129.1
1.5	-92.7	-88.4	-89.6	-87.6	-89.2	-86.0
2.5	*	-26.9	-28.8	-26.5	-28.5	-25.7
3.5	*	-4.5	-6.5	-4.6	*	-4.7

(c)

$x/b$	$\ell = 0$	1	2	3	4	5
0.5	-138.2	-134.0	-138.0	-133.0	-137.2	-131.0
1.5	-89.4	-88.7	-89.3	-88.2	-89.1	-87.1
2.5	-29.0	-20.2	-28.8	-27.0	-28.4	-26.1
3.5	-5.1	-3.6	-5.2	-4.1	-5.2	-4.5

Table Ib - The same as Ia for B1 interaction.

(a)

$x/b$	$\lambda = 0$	1	2	3	4	5
0.5	-83.0	-71.3	-84.0	-71.6	-86.9	-71.7
1.5	-53.9	-47.3	-53.7	-46.4	-53.7	-45.4
2.5	-15.4	-15.7	-15.2	-15.4	-14.8	-14.9
3.5	2.7	*	-2.8	*	-3.1	-2.1

(b)

$x/b$	$\lambda = 0$	1	2	3	4	5
0.5	-84.2	-74.3	-85.0	-74.1	-86.8	-74.1
1.5	-55.7	-51.7	-55.9	-51.1	-56.5	-51.1
2.5	-16.1	-16.6	-15.8	-16.2	-15.3	-15.8
3.5	-2.5	-2.7	-2.4	-2.8	-2.4	-3.1

(c)

$x/b$	$\lambda = 0$	1	2	3	4	5
0.5	-84.5	-76.8	-85.5	-78.4	-87.7	-77.6
1.5	-56.2	-51.6	-56.1	-50.1	-56.5	-51.9
2.5	*	-17.6	*	-17.3	*	-16.6
3.5	*	-2.8	*	*	*	-2.8

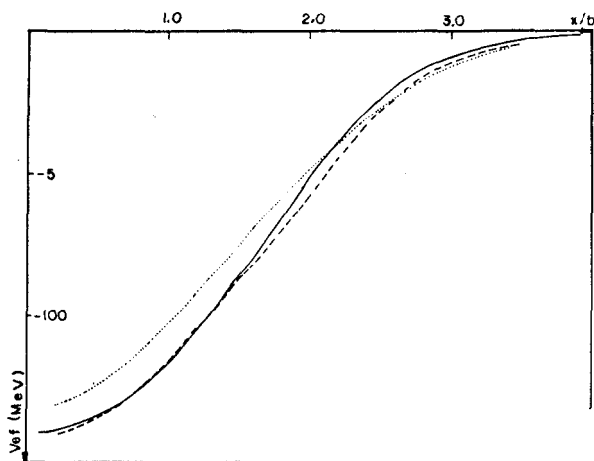


Fig.1a - Effective potentials for the  $\alpha$ - $^{16}\text{O}$  system using a  $V_2$  interaction. The full, dashed and dotted lines are, respectively,  $V_{\text{res}}^{(+)}$ ,  $\bar{V}^{(+)}$  and  $V_D$  potentials.

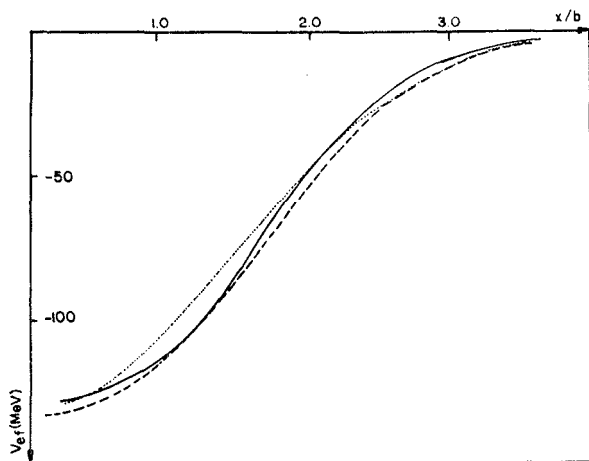


Fig.1b - The same as 1a for  $V_{\text{res}}^{(-)}$ ,  $\bar{V}^{(-)}$  and  $V_D$  potentials.

asymptotic form pushes, the Coulomb nodes away to large values of the separation coordinate. The effective potential is then free from any kind of poles in the range of the nuclear forces. The second important characteristic of such effective potentials can be seen in table 2, which shows results for the V2 interaction (the B1 interaction does not produce sharp resonances or bound states in the  $\alpha\text{-}^{16}\text{O}$  system). As in table 1 an appreciable parity dependence is still present. But, within the same parity, the dependence on angular momentum and energy is much weaker, being less than 1.5% in the most unfavourable cases. The solid lines in fig. 1 represent typical potentials,  $V_{\text{res}}^{\pm}$ , from table 2, for each parity. Notice that these potentials are slightly (a few MeV) shallower than the corresponding  $\bar{V}^{(\pm)}$  at the tail region.

Table 2 - Effective potentials (in MeV) for type V2 nuclear interaction in the resonant and bound states energies of  $\alpha\text{-}^{16}\text{O}$  system.

$x/b$	$\ell=0$ $\epsilon = -4.83$	2	4	6	8	1	3
0.5	-134.7	-134.5	-134.4	-134.2	-133.6	-124.7	-124.1
1.0	-116.6	-116.4	-116.0	-115.6	-115.0	-112.2	-111.1
1.5	-86.5	-86.4	-86.2	-86.1	-85.8	-83.2	-82.9
2.0	-50.0	-51.0	-51.1	-51.2	-51.3	-48.0	-48.4
2.5	-22.9	-22.9	-22.9	-22.9	-23.0	-24.3	-24.2
3.0	-8.1	-8.2	-8.4	-8.7	-8.9	-9.4	-9.6
3.5	-3.4	-3.4	-3.5	-3.6	-3.7	-4.0	-4.1
4.0	-1.2	-	-1.2	-1.3	-1.4	-	-1.2

The existence of potentials  $V_{\text{res}}^{(\pm)}$  with their own peculiarities suggests that parity is not the only relevant property of the RGH quantum states for the derivation of the effective potential. The necessity of working with four different potentials,  $\bar{V}^{(\pm)}$  and  $V_{\text{res}}^{(\pm)}$  will be



stressed in the next section, when we compare phase-shifts derived from different effective potentials.

**A DETERMINATION OF PHASESHIFTS. RESULTS AND DISCUSSION**

In this section we use the potentials  $\bar{v}^{(\pm)}$  and  $v_{res}^{(\pm)}$  in eq.(1) and examine phase-shifts resulting from the obtained wave function  $\chi_{\ell}(r)$ .

When a given effective potential  $V_{\ell, \epsilon}$  is obtained from a re-normalized RGM wave function  $\chi_{\ell, \epsilon}$ , solving the OCM problem with that potential is equivalent to solving the RGM equation. Nevertheless, this equivalence is lost if one uses the same potential at  $\ell' \neq \ell$  or  $\epsilon' \neq \epsilon$ . The use of a single, local, state independent potential,  $V_{ef}$ , in the OCM equation will be, however, a good approximation in the description of a set of RGM states  $\chi_{\ell', \epsilon'}$ , when

$$V_{ef} \approx V_{\ell', \epsilon'} ,$$

for any  $\ell'$  and  $\epsilon'$  in this set.

Our study of several  $V_{\ell, \epsilon}$  potentials in the previous section suggested that the space of RGM states should be splitted in four parts. For these parts the local, state independent, effective potentials  $\bar{v}^{(\pm)}$  and  $v_{res}^{(\pm)}$  were determined.

The use of these potentials in the OCM equation stresses the differences among them, showing that each one can predict the properties of those RGM states in the subspace to which it is associated, but gives bad descriptions of other RGM states.

So,  $v_{res}^{(+)}$  and  $v_{res}^{(-)}$  are able to locate accurately the sharp resonances of the system in the respective parity but they give poor approximations for the phase-shifts. To illustrate this fact we show results obtained from the solutions of the OCM equation with several effective potentials. In table 3, we give resonance energies for the partial waves  $\ell=3, \dots, 8$ , and in fig. 2 we plot  $\ell=6$  phase-shifts, a typical value of the angular momentum. While all sharp resonances are predicted to an accuracy better than 0.5 MeV, the  $\ell=6$  phase-shifts at  $\epsilon \geq 10$  MeV are appreciably different from those of the RGM. On the other hand, the

Table 3 - Energy values (in MeV) of the sharp resonances of the  $\alpha$ - $^{16}\text{O}$  system, V2 interaction; E are exact energie values coming from GCM;  $E_b$ ,  $E_c$  and  $E_d$  are, respectively, energies obtained with the potentials: a)  $V_{res}^{(+)}$ , with the corresponding parity; b)  $\bar{V}^{(\pm)}$  with the corresponding parity; c)  $V_{ap}$ ; d)  $V_D$ .

$\ell$	E	$E_a$	$E_b$	$E_c$	$E_d$
3	1.6	1.9	<0.2	1.2	0.2
5	5.3	5.7	3.3	4.5	4.1
6	2.8	2.7	<0.1	1.2	3.0
8	8.1	7.8	2.5	7.2	10.4

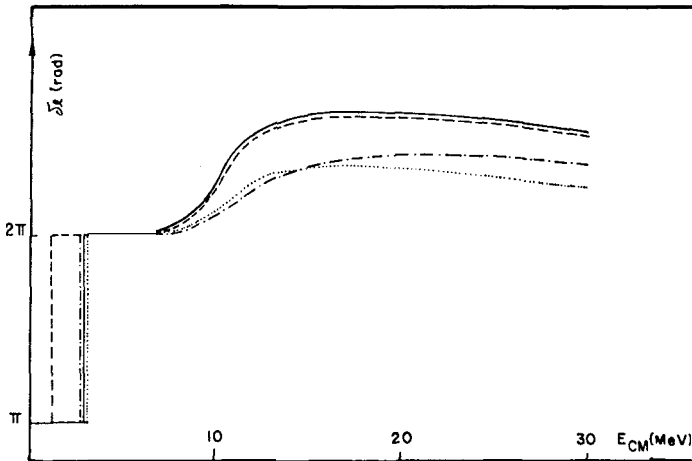


Fig.2 - Phase-shifts for the  $\ell=6$  partial wave, V2 interaction, calculated through the use in Saito's equation of  $V_{res}^{(+)}$  (dashed-dotted line),  $V_{ap}$  (dashed line) and  $V_D$  (dotted line). The full line indicates exact values.

potentials  $\bar{V}(\pm)$  reproduce phase-shifts of partial waves of the corresponding parity to a good approximation, while they are inaccurate for the calculation of resonance energies. This is illustrated in table 3 and figures 3 and 4.

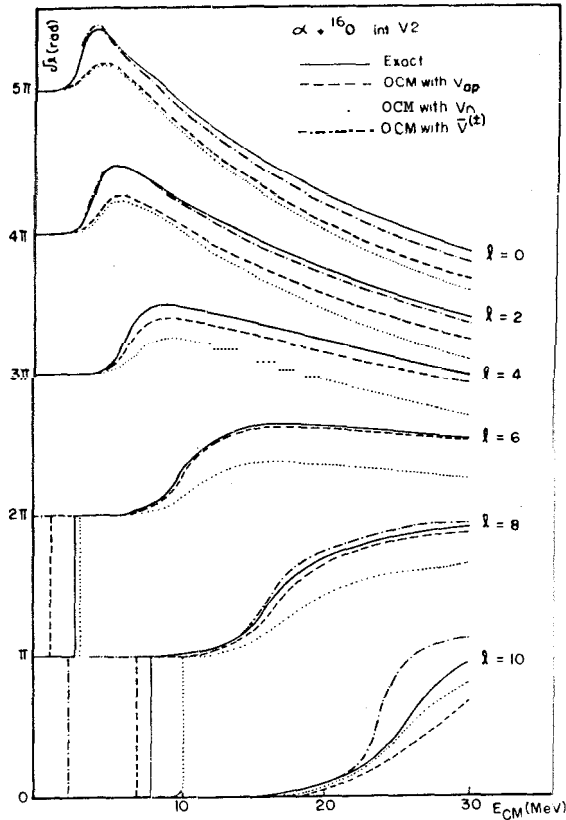


Fig.3 - Phase-shifts for even waves in  $\alpha + {}^{16}\text{O}$  system,  $V_2$  interaction. Representation is made so that  $\delta_l \rightarrow 0$  in the high energy limit<sup>14</sup>. In  $l=4$  and  $l=6$  waves, there is no distinction (except in  $l=6$  resonance) between  $\bar{V}(\pm)$  and the exact curves.

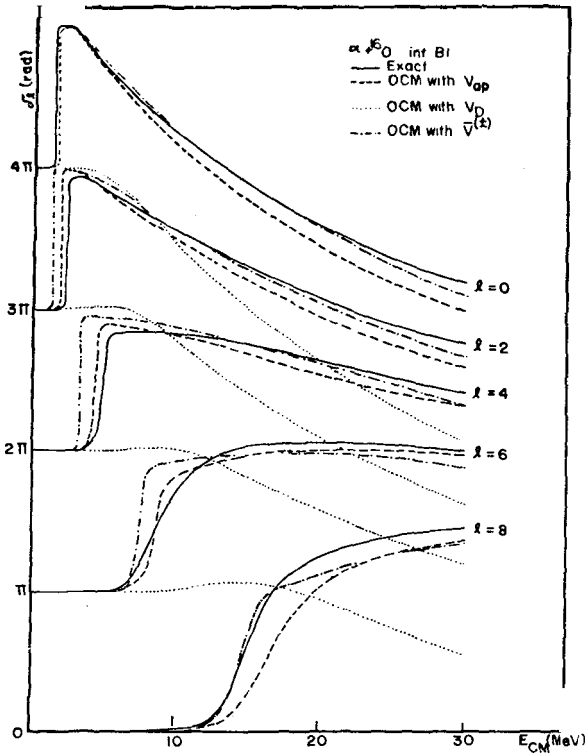


Fig.4 - Phase-shifts for even eaves of  $\alpha^{-16}\text{O}$  system, B1 interaction. The representation is the same as fig. 3.

The above results may be analysed in comparison to those obtained with a single effective potential  $V_{ap}$ , derived by the approximate method of ref. 7. Dashed lines in figs. 3 and 4 represent, respectively, phase-shifts for such potentials with a V2 interaction and with a B1 interaction. The latter is, by itself, an important result, since it shows that the approximate method works well in  $\alpha^{-16}\text{O}$  system with a B1 interaction, where the conventional OCM, with  $V_D$  (dotted lines in figs 3 and 4), fails completely. A similar situation occurs in the  $\alpha + \alpha$  system<sup>7</sup>, showing that in both cases those antisymmetrization effects ignored in the OCM approximation are much stronger for the B1 interaction. This result can also be seen comparing the RGM direct potentials to the effective potentials. While they are rather similar in calculations with a V2 interaction, they differ drastically<sup>7</sup> for the interaction B1.

An overall examination of figs. 3 and 4 reveals that although the approximate potential  $V_{ap}$  cannot do specific tasks with the same efficiency as the appropriated "specialized" potential ( $\tilde{v}^+$ ,  $\tilde{v}^-$ ,  $v_{res}^+$  or  $v_{res}^-$ ), it is globally better than each one of them alone.

In spite of the overall success of  $V_{ap}$  we should not disregard the possibility of improving the calculation of this potential. A natural step in this direction is the introduction of parity projection in eq. (4). This would lead to different potentials for each parity, as it is suggested in our study of  $V_{\ell,\epsilon}$ . This was, however, done in ref. 9, without any significant improvement of the results.

A possible way to improve the derivation of  $V_{ap}$  without introducing further complications is to include off-diagonal GCM kernels\*  $\tilde{H}(\vec{\alpha}, \vec{\alpha}')$  in the mesh to which eq. (4) is fitted. This can be done rather easily if we keep  $\vec{\alpha}$  parallel to  $\vec{\alpha}'$ . We followed this procedure and the resulting effective potentials showed an appreciable dependence on the choice of the mesh. The mesh of table 4, for example, led to the potential shown in fig. 5 and to the phase-shifts of fig. 6. This particular mesh is very favourable for the description of  $R=0$  but it gets progressively worse for higher partial waves. Choosing other off-diagonal meshes would improve the description of the other waves and give poorer  $s$ -wave phase-shifts. In conclusion we should say that the overall agreement with the RGM phase-shift: is not significantly improved.

It should also be pointed out that although the two potentials of fig. 5 are rather different at small separations they are rather similar at the tail, where they are also close to  $\tilde{v}^+$ .

Table 4 - Mesh used in non-diagonal GCM kernel elements. Values are in fm.

$\alpha_1$	2.0	2.0	2.0	2.0	4.0	4.0	4.0	4.0	...	8.0	8.0	8.0	8.0
$\alpha_2$	2.0	2.5	3.0	3.5	4.0	5.0	6.0	7.0	...	8.0	10.0	12.0	14.0

\* Notice that eq. (4) is transformed<sup>7</sup> into the GCM space before the effective potential is determined as to fit it in a mesh of diagonal values.

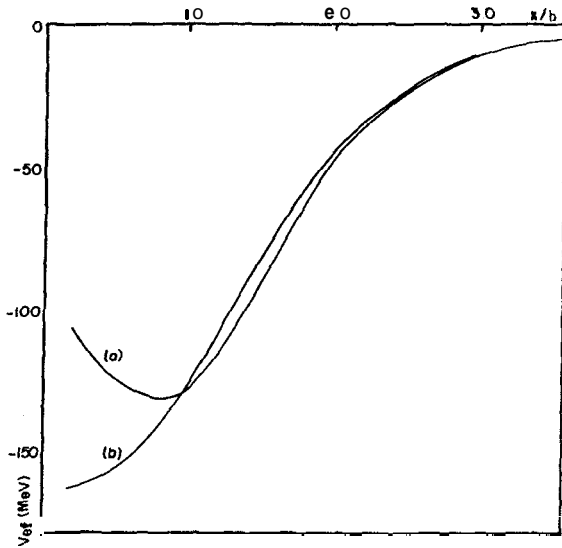


Fig.5 - Effective potentials obtained by the approximate method for V2 interaction, using GCM kernel elements: a) only diagonals; b) including non-diagonals given by the mesh of table 4.

5. CONCLUSION

We have studied the effects of the Pauli principle in  $\alpha^{-16}O$  scattering with the help of the OCM and the RGM. A method to derive effective potentials for the OCM from RGM wave functions was developed, and a technique to eliminate poles associated to the orthogonality to forbidden states was introduced.

This method was applied to  $\alpha^{-16}O$  scattering with V2 and B1 nucleon-nucleon interactions. The resulting effective potentials showed a pronounced dependence on parity and a weak dependence on energy and angular momentum in potentials for the same parity. It was also shown that effective potentials derived from RGM resonant or bound states are appreciably different. On the basis of these results the introduction of four different effective potentials,  $\bar{V}^{(\pm)}$  and  $V_{res}^{(\pm)}$  was suggested. OCM phase-shifts with  $\bar{V}^{(\pm)}$  and  $V_{res}^{(\pm)}$  were calculated and the results were compared to exact RGM phase-shifts and to OCM phase-shifts obtained from the approximate potential  $V_{ap}$  of ref. 7.

Although the "specialized" potentials  $\bar{V}^{(\pm)}$  and  $V_{res}^{(\pm)}$  were more efficient for specific tasks (like resonance energy or phase-shift cal-

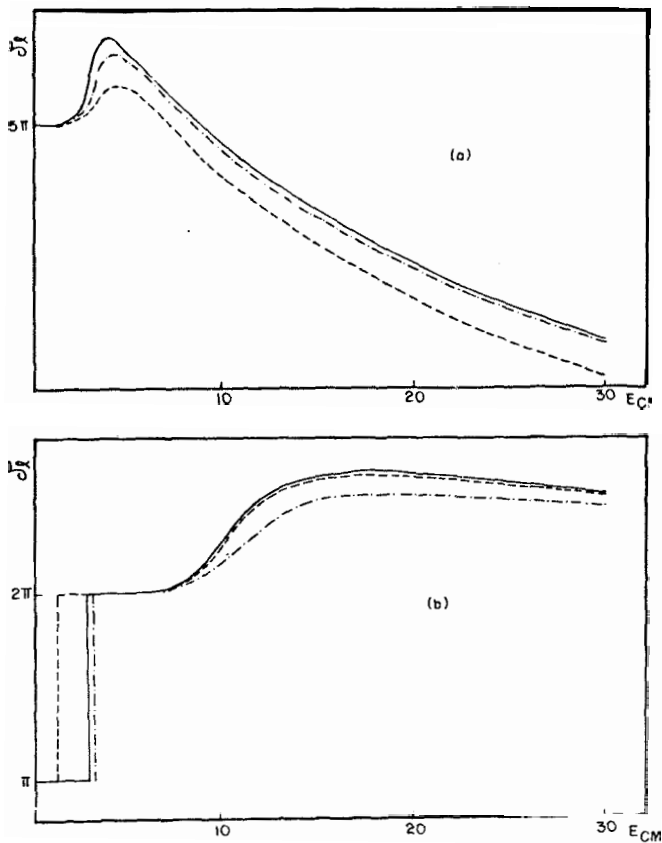


Fig.6 - Comparison between phase-shifts obtained with the "diagonal" potential (dashed lines) and the "non-diagonal" one (dashed-dotted lines) for the waves: (a)  $l=0$ ; (b)  $l=6$ . Full lines represent exact values.

culations for a given parity),  $V_{ap}$  was shown to have the best overall performance.

Further investigations involving the approximate method for deriving effective potentials and studies of heavier systems are in progress.

#### REFERENCES

1. Y.C.Tang *et al*, Phys. Rep. 47, 169 (1979)
2. C.W.Wong, Phys. Rep. 15, 183 (1975).
3. Y.Suzuki, Nucl. Phys. 408, 40 (1983).
4. H.R.Fiebig and W.Timm, Phys. Rev. C26, 2496 (1982).
5. S.Saito, Progr. Theor. Phys. 42, 705 (1969); H.Friedrich, Phys.Rep. 74, 209 (1981).
6. B.Buck *et al*, Nucl. Phys. A275, 246 (1977).
7. H.Friedrich and L.F.Canto, Nucl.Phys.A291, 249 (1977).
8. D.Wintge *et al*, Nucl. Phys. A408, 259 (1983).
9. A.M.Breitschaft *et al*, Rev.Bras.Física, 13, 328 (1983).
10. H.Friedrich, Nucl. Phys. A294, 81 (1978).
11. L.F.Canto and D.M.Brink, Nucl. Phys. A279, 85 (1977).
12. A.B.Volkov, Nucl. Phys. 74, 33 (1965).
13. D.M.Brink and E.Boeker, Nucl. Phys. A 91, 1 (1967).
14. M.J.Englefield and H.J.M.Shoukry, Prog.Theor.Phys. 52, 1554 (1974).

#### Resumo

Métodos microscópicos "exatos" como o RGM (Método do Grupo Ressonante) e o GCM (Método da Coordenada Geradora) e métodos aproximados como o OCM (Modelo da Condição de Ortogonalidade) são empregados para se estudar os efeitos do Princípio de Pauli no espalhamento elástico  $\alpha$ - $^{16}\text{O}$ . Um método de se obter potenciais efetivos "exatos" para o OCM é criado. Esses potenciais, obtidos da função de onda do RGM tornam o OCM idêntico ao RGM e têm a vantagem de serem livres de polos associados aos estados proibidos. Usando forças nucleon-nucleon  $V_2$  e  $B_1$  cálculos numéricos são feitos na faixa de energias 0-30 MeV. Os potenciais e as defasagens resultantes são comparados aos obtidos do método aproximado sugerido por Friedrich e Canto. O problema de se procurar um potencial local, independente de estado, para o OCM é discutido.